A. Sengupta
R. Mahalakshmi
N. Shamala
P. Balaram

Aromatic interactions in tryptophan-containing peptides: crystal structures of model tryptophan peptides and phenylalanine analogs*

Authors' affiliations:

A. Sengupta and N. Shamala, Department of Physics, Indian Institute of Science, Bangalore 560 012, Karnataka, India

R. Mahalakshmi and P. Balaram, Molecular Biophysics Unit, Indian Institute of Science, Bangalore 560 012, Karnataka, India

Correspondence to:
N. Shamala
Department of Physics
Indian Institute of Science
Bangalore 560 012
India
Tel.: 91-80-22932856
Fax: 91-80-23602602/91-80-23600683
E-mail: shamala@physics.iisc.ernet.in

Key words: aromatic interactions; crystal structures; peptide conformations; superhelical structure; tryptophan peptides

Abstract: The crystal structures of the peptides, Boc-Leu-Trp-Val-OMe (**1**), Ac-Leu-Trp-Val-OMe (**2a** and 2b), Boc-Leu-Phe-Val-OMe (**3**), Ac-Leu-Phe-Val-OMe (**4**), and Boc-Ala-Aib-Leu-Trp-Val-OMe (**5**) have been determined by X-ray diffraction in order to explore the nature of interactions between aromatic rings, specifically the indole side chain of Trp residues. Peptide **1** adopts a type I β-turn conformation stabilized by an intramolecular 4 → 1 hydrogen bond. Molecules of **1** pack into helical columns stabilized by two intermolecular hydrogen bonds, Leu(1)NH…O(2)Trp(2) and IndoleNH…O(1)Leu(1). The superhelical columns further pack into the tetragonal space group $P4_3$ by means of a continuous network of indole–indole interactions. Peptide **2** crystallizes in two polymorphic forms, $P2_1$ (**2a**) and $P2_12_12_1$ (**2b**). In both forms, the peptide backbone is extended, with antiparallel β-sheet association being observed in crystals. Extended strand conformations and antiparallel β-sheet formation are also observed in the Phe-containing analogs, Boc-Leu-Phe-Val-OMe (**3**) and Ac-Leu-Phe-Val-OMe (**4**). Peptide **5** forms a short stretch of 3_{10}-helix. Analysis of aromatic–aromatic and aromatic–amide interactions in the structures of peptides, **1**, **2a**, **2b** are reported along with the examples of 14 Trp-containing peptides from the Cambridge Crystallographic Database. The results suggest that there is no dramatic preference for a preferred orientation of two proximal indole rings. In Trp-containing peptides specific orientations of the indole ring, with respect to the preceding and succeeding peptide units, appear to be preferred in β-turns and extended structures.

Abbreviations: Aib, α-amino isobutyric acid; Boc, tert-butyloxycarbonyl; OMe, methyl ester; Ac, acetyl; DCC/HOBT, dicyclohexylcarbodiimide/1-hydroxybenzotriazole; MPLC, medium pressure liquid chromatography.

Dates:
Received 19 August 2004
Revised 29 September 2004
Accepted 10 October 2004

*Dedicated to the memory of Murray Goodman.

To cite this article:
Sengupta, A., Mahalakshmi, R., Shamala, N. & Balaram, P. Aromatic interactions in tryptophan-containing peptides: crystal structures of model tryptophan peptides and phenylalanine analogs.
J. Peptide Res., 2005, **65**, 113–129.
DOI 10.1111/j.1399-3011.2004.00191.x

Introduction

The folded structures of peptides and proteins are stabilized by networks of backbone hydrogen bonds and a multitude of weak interactions involving the side chains of amino acid residues. Trp is unique among the 20 amino acid residues found in proteins because its large indole side chain can participate in the formation of nonpolar clusters and also in hydrogen bonding, with the indole NH-group serving as a donor. In addition, the indole ring can serve as an acceptor for weak NH…π hydrogen bonds (1,2) and also participate in weak electrostatic interactions involving the quadrupoles of the aromatic ring (3–5). Trp residues play an important role in membrane proteins invariably occurring at the lipid–water interface, as a consequence of the amphipathic nature of indole side chains (6–10). The importance of Trp in formation of hydrophobic clusters, which may be important in the folding pathway of proteins, has been emphasized in a recent study of hen lysozyme (11). Cross-strand interactions between facing Trp residues have been advanced as a means of stabilizing designed β-hairpin structures (12). Several analyses of protein crystal structures have attempted to dissect the nature of stabilizing interactions involving the indole side chain of the Trp residue (13–15). In order to systematically analyze interactions involving the indole side chain of Trp we have embarked on program of

Table 1. **Crystal and diffraction parameters for peptides, 1–5**

	Peptide **1**	Peptide **2a**	Peptide **2b**	Peptide **3**	Peptide **4**	Peptide **5**
Empirical formula	$C_{28}H_{42}N_4O_6$	$C_{25}H_{36}N_4O_5$	$C_{25}H_{36}N_4O_5$	$C_{26}H_{41}N_3O_6$	$C_{23}H_{35}N_3O_5$	$C_{35}H_{50}N_6O_8{\cdot}2H_2O$
Crystal habit	Colorless rod	Colorless rod	Colorless rod	Colorless knife	Colorless needle	Colorless plate
Crystal size (mm)	0.54 × 0.1 × 0.05	0.6 × 0.25 × 0.18	0.58 × 0.17 × 0.1	0.6 × 0.4 × 0.24	0.5 × 0.04 × 0.01	0.45 × 0.4 × 0.14
Crystallizing solvent	Methanol/water	Methanol/water	Methanol/water	Ethanol/water	Ethanol/water	Methanol/water
Space group	$P4_3$	$P2_1$	$P2_12_12_1$	C2	$P2_12_12_1$	$P2_1$
Cell parameters						
a (Å)	14.6979 (10)	10.966 (3)	9.533 (6)	31.318 (8)	9.514 (8)	9.743 (3)
b (Å)	14.6979 (10)	9.509 (2)	14.148 (9)	10.022 (3)	13.563 (11)	22.807 (7)
c (Å)	13.9749 (8)	14.130 (3)	19.527 (13)	9.657 (3)	20.046 (17)	10.106 (3)
β (deg)	90	104.941 (4)	90	107.409 (4)	90	105.730 (6)
Volume (Å^3)	3019.0 (5)	1423.6 (6)	2634 (3)	2892.2 (13)	2587 (4)	2161.6 (12)
Z	4	2	4	4	4	2
Molecules/asymmetric unit	1	1	1	1	1	1
Co-crystallized solvent	None	None	None	None	None	Two H_2O
Molecular weight	530.66	472.58	472.58	491.62	433.54	718.84
Density (g/cm^3) (cal)	1.168	1.102	1.192	1.129	1.113	1.104
F(000)	1144	508	1016	1064	936	772
Radiation	MoK_α	MoK_α	MoK_α	MoK_α	MoK_α	MoK_α
Temperature (°C)	20	20	20	20	20	20
2θ maximum (°)	54.76	54.64	52.68	54.80	46.50	54.8
Measured reflection	24 401	11 115	19 056	9345	15 649	17 103
R_{int}	0.0507	0.0306	0.0207	0.0234	0.0234	0.0737
Independent reflection	6372	5668	4928	5656	3711	8638
Observed reflections [$\|F\| > 4\sigma(F)$]	4654	4408	4499	4855	2761	5654
Final *R* (%)/wR_2 (%)	7.09/15.10	6.59/18.17	4.44/12.0	5.96/15.54	8.55/17.77	7.91/18.53
Goodness-of-fit (S)	1.121	1.065	1.099	1.054	1.126	1.066
$\Delta\rho_{max}$(eÅ^{-3})/$\Delta\rho_{min}$ (eÅ^{-3})	0.401/−0.119	0.390/−0.244	0.191/−0.310	0.317/−0.285	0.259/−0.184	0.533/−0.278
Number of restraints/parameters	1/415	3/323	0/403	5/329	0/292	6/470
Data-to-parameter ratio	11.2 : 1	13.6 : 1	11.1 : 1	14.7 : 1	9.4 : 1	12 : 1

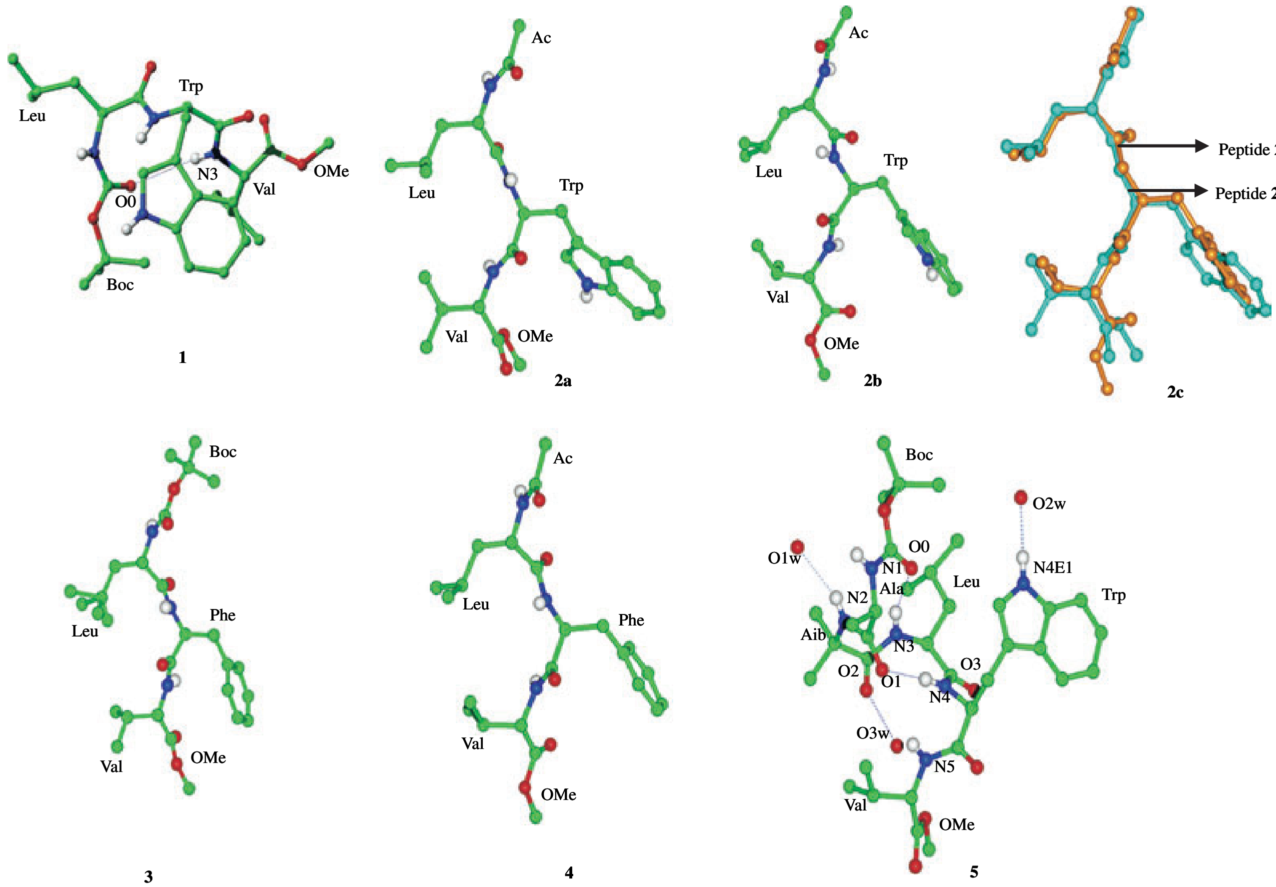

Figure 1. Molecular conformation of peptides **1–5**. Peptide **2c**, represents the superposition of two polymorphs of Ac-Leu-Trp-Val-OMe. Hydrogen bonds are shown by dotted lines.

crystal structure determination of synthetic Trp-containing peptides.

We describe in this report the crystal structures of the following peptides: Boc-Leu-Trp-Val-OMe (peptide **1**), Ac-Leu-Trp-Val-OMe (peptide **2a**), Ac-Leu-Trp-Val-OMe (peptide **2b**).

In addition analogs of **1** and **2** in which Trp is replaced by Phe, are also described: Boc-Leu-Phe-Val-OMe (peptide **3**), Ac-Leu-Phe-Val-OMe (peptide **4**). Boc-Ala-Aib-Leu-Trp-Val-OMe (peptide **5**).

The structures provide a view of both inter- and intramolecular interactions involving the Trp side chains in three distinct secondary structure contexts. Peptide **1** adopts a folded β-turn structure, peptide **2a** and **2b** are extended and aggregates to form an antiparallel β-sheet in crystal, while peptide **5** folds to a short stretch of 3_{10}-helix. Indole–indole and indole–amide interactions observed in the structure of peptides, **1**, **2a** and **2b** are analyzed together with examples of Trp-containing peptides extracted from the Cambridge Crystallographic Database.

Experimental Procedures

Peptide synthesis

All peptides were synthesized by standard solution phase chemistry using Boc (tert-butyloxycarbonyl) and methyl esters as protecting groups for the N- and C-termini, respectively. Coupling reactions were mediated by dicyclohexylcarbodiimide/1-hydroxybenzotriazole (DCC/HOBT). The final peptides were purified by medium pressure liquid chromatography (MPLC) on a C_{18} column (40–60 micron pore size) using methanol-water gradients. Acetylation of the purified peptides was carried out after acidolytic cleavage of the Boc-group and subsequent treatment of the free peptide with acetic anhydride under basic conditions. The homogeneity and identity of the peptides were established by high-performance liquid chromatography using methanol-water gradients and 400 MHz ^{1}H one-dimensional nuclear magnetic resonance (1D NMR) spectra and mass spectrometry ($M_H^+ = 531.3$, $M_{Na}^+ = 553.3$, $M_{cal} = 530.0$ for peptide **1**; $M_H^+ = 473.4$, $M_{Na}^+ = 495.4$,

Table 2. **Torsion angles[a] (deg) of peptides, 1–5**

Residues	ϕ	ψ	ω	χ^1	χ^2
Peptide **1**					
Leu(1)	−76.8[b]	−11.6	−177.1	−57.3	−57.2, 177.1
Trp(2)	−91.0	−8.8	−170.7	53.4	80.6, −99.1
Val(3)	−62.7	150.4[c]	175.0[d]	67.8, −164.1	
Peptide **2a**					
Leu(1)	−110.9[b]	131.0	173.0	178.8	68.3, −166.9
Trp(2)	−136.4	114.0	−178.4	−176.9	41.8, −138.6
Val(3)	−104.2	−44.5[c]	−176.9[d]	−65.1, 179.4	
Peptide **2b**					
Leu(1)	−109.3[b]	133.5	173.4	−176.4	66.8, −168.8
Trp(2)	−135.1	114.0	−177.5	172.2	63.4, −119.0
Val(3)	−134.3	172.6[c]	−178.8[d]	55.8, −69.3	
Peptide **3**					
Leu(1)	−99.2[b]	127.3	167.8	−179.6	−80.3, 135.2, 49.7, −149.5
Phe(2)	−124.3	135.6	168.8	175.7	78.5, −94.6
Val(3)	−147.3	143.7[c]	179.7[d]	59.6, −172.6	
Peptide **4**					
Leu(1)	−106.8[b]	133.1	169.7	−178.5	73.5, −160.0
Phe(2)	−139.8	111.9	−178.3	−174.6	73.7, −107.7
Val(3)	−125.7	173.7[c]	176.4[d]	57.8, −67.0	
Peptide **5**					
Ala(1)	−58.7[b]	−28.1	−178.2		
Aib(2)	−50.2	−37.1	−173.9		
Leu(3)	−77.2	−14.2	−162.9	−60.6	−39.5, −165.4
Trp(4)	−123.2	4.8	177.0	−64.0	−67.4, 110.9
Val(5)	−92.5	−19.2[e]	−175.5[f]	−62.6, 65.1	

a. The torsion angles for rotation about bonds of the peptide backbone (ϕ,ψ and ω) and about bonds of the amino acid side chains (χ^1,χ^2) as suggested by the IUPAC-IUB Commission on Biochemical Nomenclature (*Biochemistry*, 1970, **9**, 3471–3479).
b. C′(0)–N(1)–C$^\alpha$(1)–C′(1).
c. N(3)–C$^\alpha$(3)–C′(3)–O(OMe).
d. C$^\alpha$(3)–C′(3)–O(OMe)–C(OMe).
e. N(5)–C$^\alpha$(5)–C′(5)–O(OMe).
f. C$^\alpha$(5)–C′(5)–O(OMe)–C(OMe).

$M_{cal} = 472.0$ for peptides **2a** and **2b**; $M_H^+ = 492.3$, $M_{Na}^+ = 514.4$, $M_{cal} = 491.0$ for peptide **3**; $M_H^+ = 433.2$, $M_{Na}^+ = 455.8$, $M_{cal} = 432.0$ for peptide **4**; $M_{Na}^+ = 709.2$, $M_K^+ = 725.5$, $M_{cal} = 686.0$ for peptide **5**).

X-ray diffraction

Single crystals, of peptides **1–5** suitable for X-ray diffraction, were grown by slow evaporation from methanol/water mixtures (for peptides **1**, **2a**, **2b**, and **5**) and ethanol/water mixtures (for peptides **3** and **4**). The X-ray intensity data for peptide crystals, **1–5**, were collected at room temperature on a Bruker AXS (Madison, WI, USA) SMART APEX CCD diffractometer with graphite monochromated MoK$_\alpha$ (λ = 0.71073 Å) radiation. Peptide **2**, crystallized in two polymorphic forms (**2a** and **2b**). The structures of peptides, **1–5**, were determined by direct phase determination using SHELXS-97 (16). Refinement for all the six structures were carried out with a full matrix anisotropic least-square method using SHELXL-97 (17). In peptide **5**, three water sites were observed from the difference Fourier map during the refinement. For peptide **1**, hydrogen atoms attached to one of the methyl groups of the tert-butyloxycarbonyl moiety (Boc CoT1); Leu(1) N1, CA, CB, CG; Trp(2) N2, CA, CB, CD1, NE1, CZ3, CE3; Val(3) N3, CA were located from

Table 3. **Hydrogen bond parameters of peptides, 1–5**

Type	Donor (D)	Acceptor (A)	D…A (Å)	H…A (Å)	C=O…H (°)	C=O…D (°)	OH…D (°)
Peptide **1**							
Intramolecular							
4 → 1	N(3)	O(0)	3.623	2.815	111.9	112.3	172.4
Intermolecular[p]	N(1)	O(2)[a]	2.877	2.118	138.2	141.0	169.3
	N(2E1)	O(1)[a]	2.985	2.157	160.7	155.3	157.3
Peptide **2a**							
Intermolecular[p]	N(1)	O(2)[b]	2.923	2.193	152.5	153.6	172.2
	N(2)	O(1)[c]	2.847	1.968	152.2	153.9	173.4
	N(2E1)	O(3)[d]	2.914	2.074	150.0	153.8	162.4
	N(3)	O(0)[b]	2.838	2.146	147.5	149.9	170.3
Peptide **2b**							
Intermolecular[p]	N(1)	O(2)[e]	2.913	2.097	146.8	150.6	165.1
	N(2)	O(1)[f]	2.948	2.108	144.9	146.5	163.6
	N(2E1)	O(3)[g]	3.211	2.444	168.4	158.3	140.9
	N(3)	O(0)[e]	2.882	2.050	139.2	144.5	160.6
Peptide **3**							
Intermolecular[p]	N(1)	O(3)[h]	2.970	2.164	166.3	164.6	173.7
	N(2)	O(2)[i]	2.942	2.193	158.4	159.4	174.2
	N(3)	O(1)[h]	2.956	2.147	156.2	158.2	162.4
Peptide **4**							
Intermolecular[p]	N(1)	O(2)[j]	2.935	2.078	153.2	152.3	176.7
	N(2)	O(1)[k]	2.973	2.083	142.5	143.1	169.7
	N(3)	O(0)[j]	2.879	2.069	135.0	141.2	158.3
Peptide **5**							
Intramolecular							
4 → 1[p]	N(3)	O(0)	3.149	2.336	126.0	129.9	157.7
4 → 1[p]	N(4)	O(1)	2.938	2.092	123.6	125.9	167.8
5 → 1	N(5)	O(1)	3.458	2.936	165.3	176.3	120.9
Intermolecular[p]	N(1)	O(3)[l]	2.938	2.116	162.3	167.4	159.5
	N(2)	O1W	3.057	2.231			161.1
	N(4E1)	O2W[o]	2.907	2.121			151.6
Solvent[p]	O3W[o]	O(2)	2.865				
	O1W	O(4)[m]	2.847				
	O1W	O(3)	2.837				
	O2W[o]	O(5)[n]	3.021				
	O3W[o]	O1W	2.969				

a. Symmetry related by ($-x + 1$, $-y$, $z - 1/2$).
b. Symmetry related by ($-x$, $y - 1/2$, $-z + 1$).
c. Symmetry related by ($-x$, $y + 1/2$, $-z + 1$).
d. Symmetry related by ($-x$, $y - 1/2$, $-z + 2$).
e. Symmetry related by ($x - 1/2$, $-y + 1/2$, $-z + 2$).
f. Symmetry related by ($x + 1/2$, $-y + 1/2$, $-z + 2$).
g. Symmetry related by ($x + 1/2$, $-y + 3/2$, $-z + 2$).
h. Symmetry related by ($-x + 2$, y, $-z + 1$).
i. Symmetry related by ($-x + 2$, y, $-z + 2$).
j. Symmetry related by ($x + 1/2$, $-y + 1/2$, $-z + 2$).
k. Symmetry related by ($x - 1/2$, $-y + 1/2$, $-z + 2$).
l. Symmetry related by (x, y, $z + 1$).
m. Symmetry related by ($x + 1$, y, $z + 1$).
n. Symmetry related by ($-x + 1$, $y - 1/2$, $-z$).
o. The occupancy of O2W = O3W = 0.5.
p. These are acceptable hydrogen bonds.

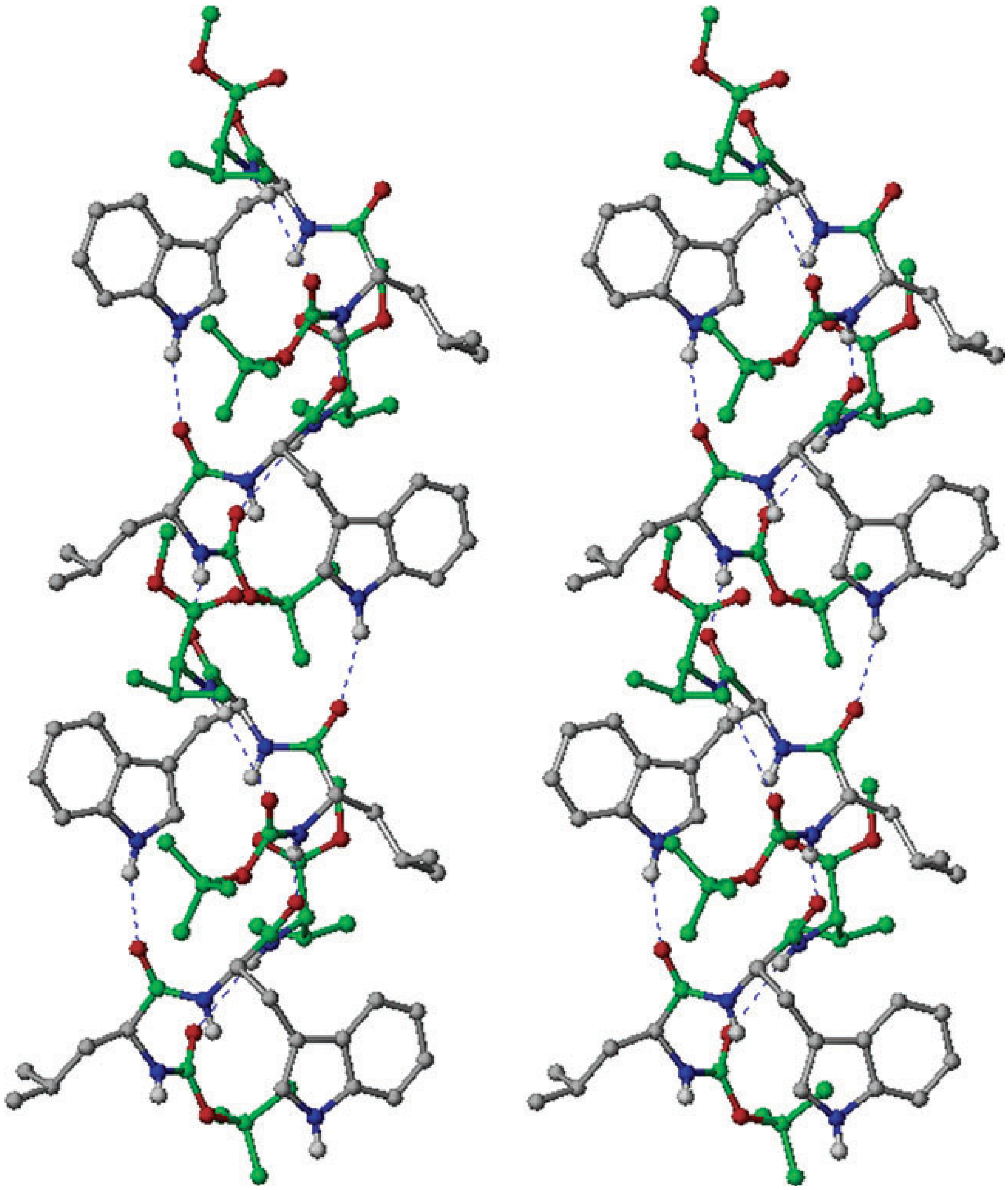

Figure 2. Stereo view of superhelical molecular packing of peptide **1**, Boc-Leu-Trp-Val-OMe.

difference Fourier maps and refined isotropically. The rest of the hydrogen atoms were fixed geometrically in idealized positions and refined as riding over the heavier atom to which they are bonded. For peptides **2a**, **3**, and **4**, those hydrogen atoms attached to nitrogens were located from difference Fourier maps and refined isotropically. The rest of the hydrogen atoms of these peptides and all the hydrogen atoms of peptide **5** were fixed geometrically in the idealized positions and refined as riding over the heavier atom to which they were bonded. For peptide **2b**, all hydrogens except for protecting groups (Boc, OMe) and Leu(1) CD1, CD2 carbons were located from difference Fourier maps and refined isotropically. The remaining hydrogen atoms were fixed geometrically using the riding atom model. All the relevant crystallographic data collection parameters and structure refinement details for the six peptides are summarized in Table 1. CCDC-220248 **1**, CCDC-247188 **2a**, CCDC-247187 **2b**, CCDC-247185 **3**, CCDC-247189 **4**, and CCDC-247186 **5** contains the supplementary crystallographic data for this paper. These data can be obtained free-of-charge via http://www.ccdc.cam.ac.uk/conts/retrieving.html (or from the Cambridge Crystallographic Data Centre, 12 Union Road, Cambridge CB_2 $_1EZ$, UK; fax: (+44)-1223-336-033; or e-mail: deposit@ccdc.cam.ac.uk).

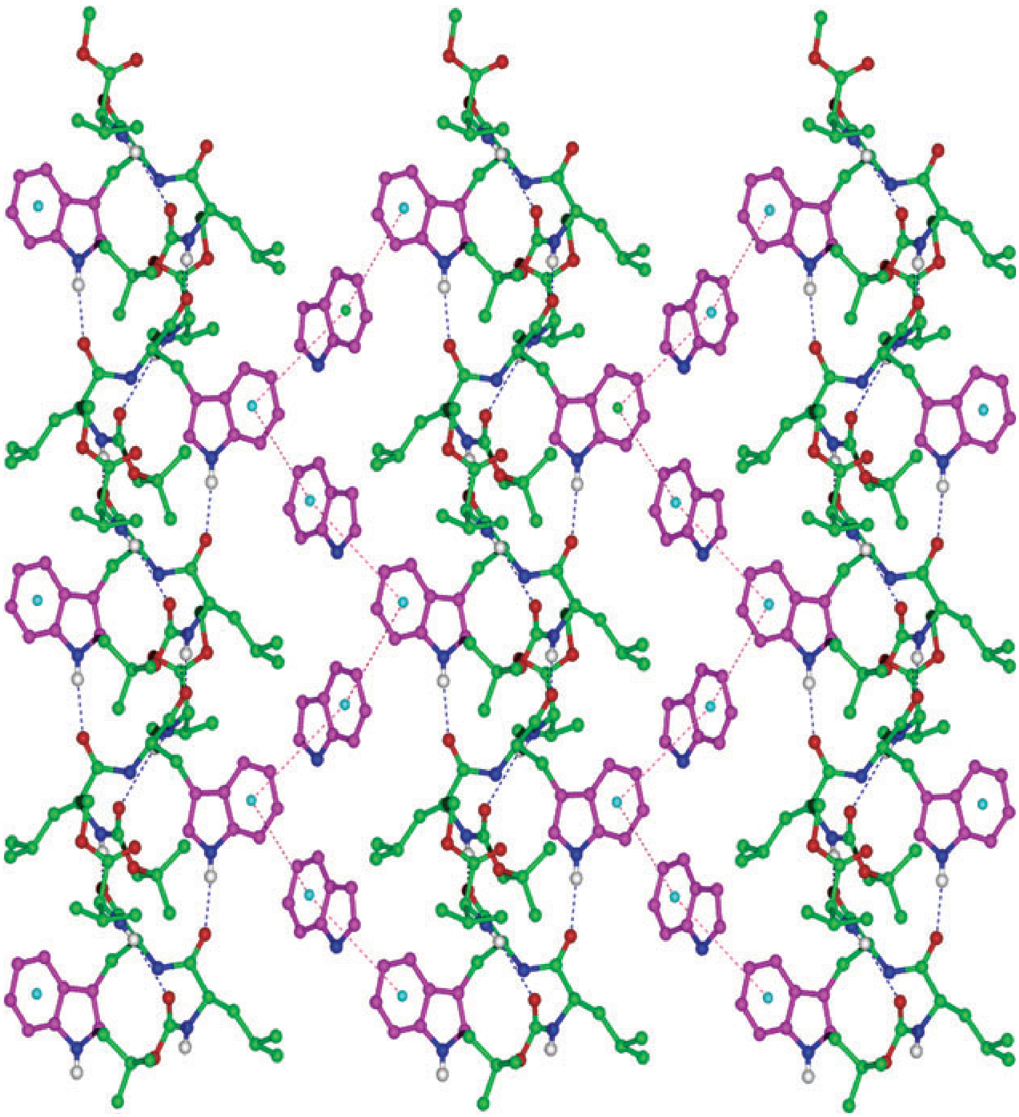

Figure 3. Three aligned superhelical peptide columns viewed down the *b*-axis, illustrating the Trp–Trp interactions along the *c*-axis. Dotted lines show hydrogen bonds and the short Trp–Trp distance (5.63 Å). The centroid of the 6-membered ring is shown.

Figure 4. Two views of the unit cell indicating Trp–Trp interactions 1–2, 2–3, 3–4 highlighting the left-handed screw, generating 4_3 symmetry.

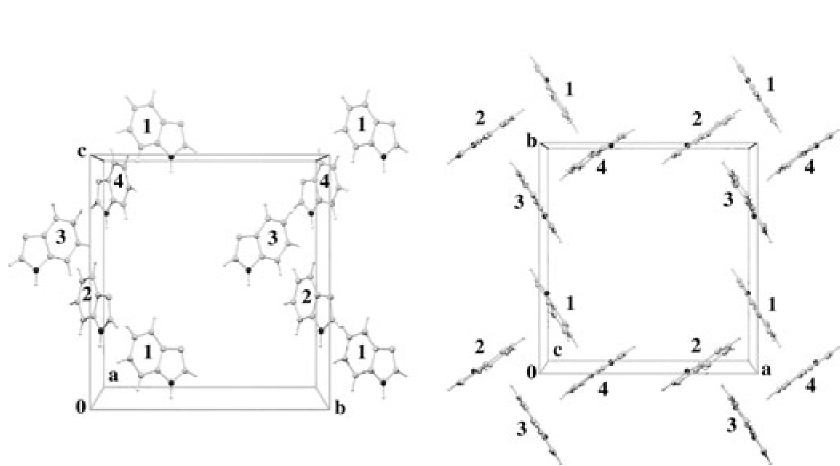

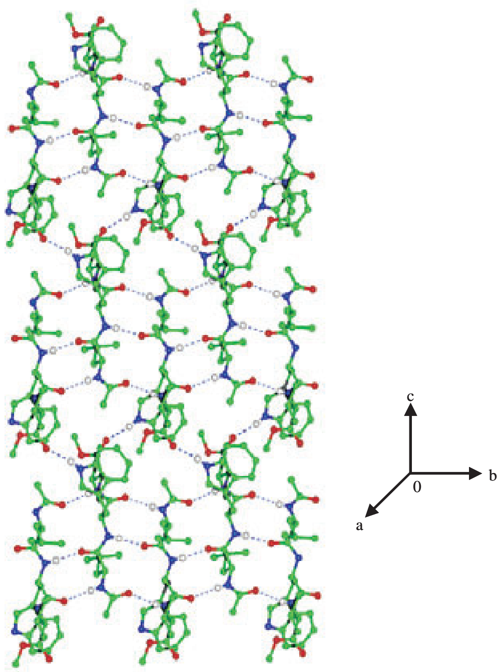

2A

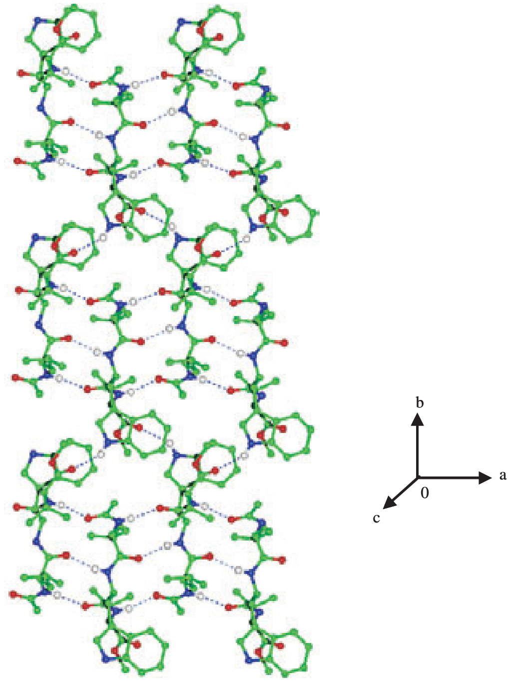

2B

Figure 5. Packing of two polymorph of peptide, Ac-Leu-Trp-Val-OMe (2A and 2B) forming an antiparallel β-sheet through intermolecular hydrogen bond.

Results

Boc-Leu-Trp-Val-OMe (1)

Figure 1 shows the molecular conformation of peptide **1**. The relevant backbone and side chain torsion angles are listed in Table 2 and hydrogen bond parameters in Table 3. Peptide **1** adopts a type I β-turn conformation with the ϕ-, ψ-values of Leu(1) and Trp(2) lying in the right-handed α-helical regions of ϕ,ψ space. β-Turns are usually characterized by the presence of a $4 \rightarrow 1$ hydrogen bond involving the C=O group of residue (i) and the NH-group of residue ($i + 3$), with ($i + 1$) and ($i + 2$) being the two corner residues of the turn segments. The N…O distance corresponding to the potential NH…O hydrogen bond [Boc C(0′)…HNVal(3)] is 3.623 Å, which is somewhat long for a stabilizing interaction. Such long hydrogen bonds are not uncommon in peptide β-turns (18). The Trp side chain is folded over the two segments with a *gauche* conformation about C^{α}–C^{β} bond ($\chi^1 = 53.4°$). A similar folding pattern for the tripeptide backbone has been observed in crystals of two tripeptides containing a central Trp residue of sequences, Boc-Gly-Trp-Ala-O^{t}Bu (19) and Z-Aib-Trp-Aib-OMe (20).

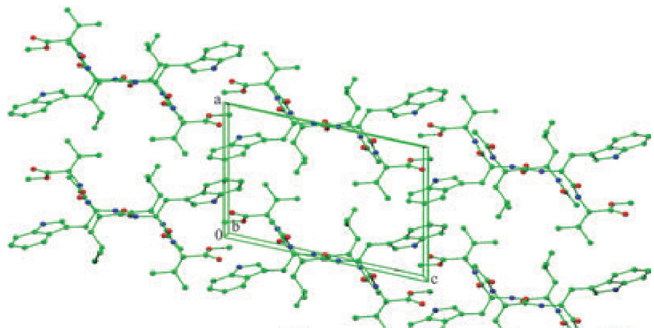

2A

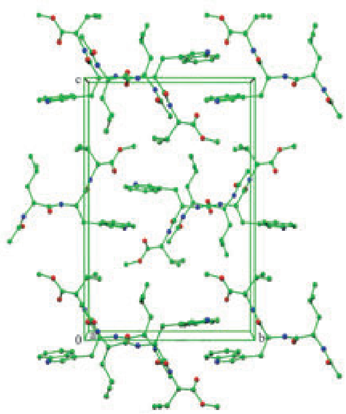

2B

Figure 6. Another view of packing of two polymorph of peptide, Ac-Leu-Trp-Val-OMe (2A and 2B), shows aromatic interactions.

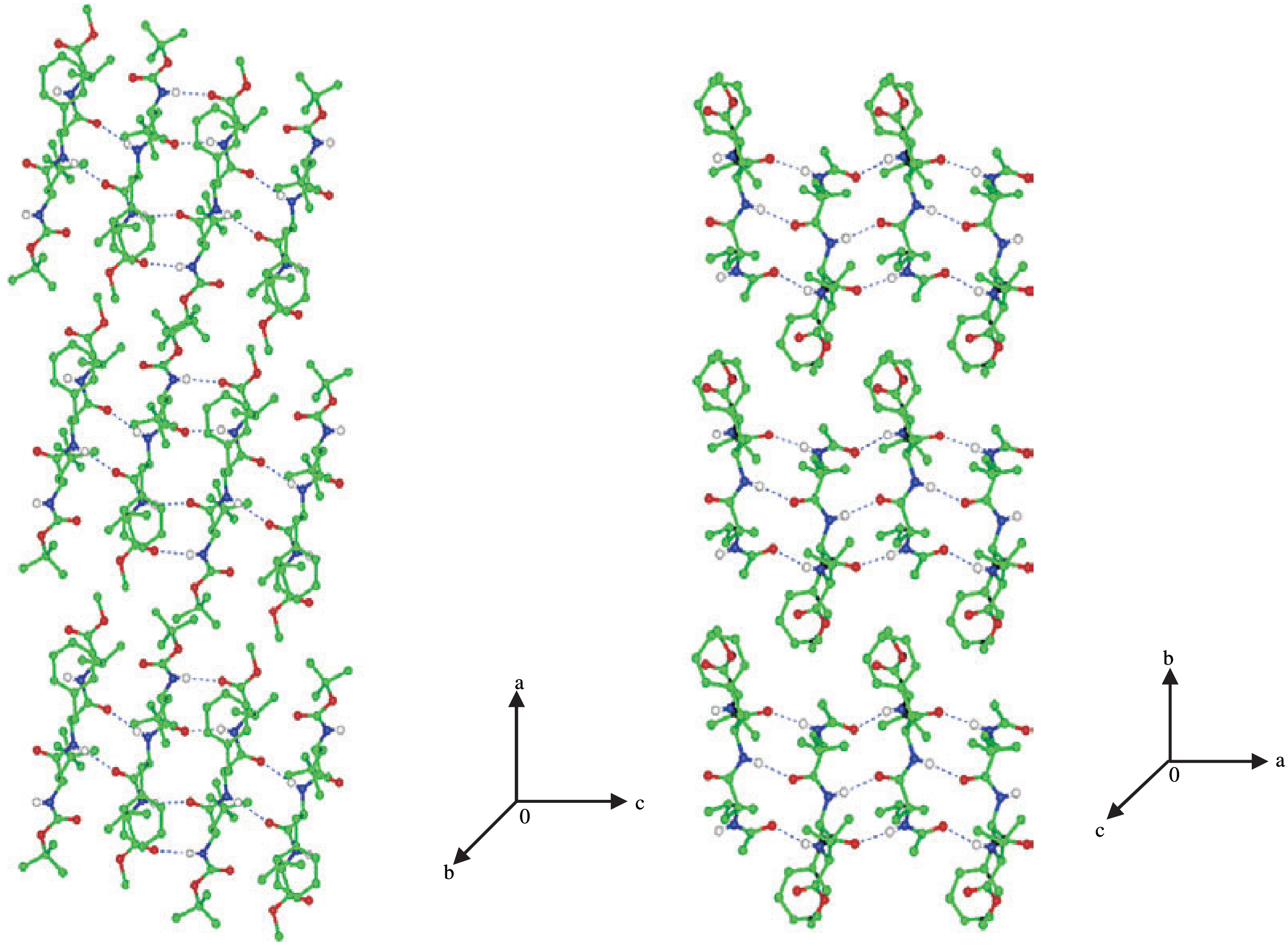

3

4

Figure 7. Packing of peptides, Boc-Leu-Phe-Val-OMe (**3**) and Ac-Leu-Phe-Val-OMe (**4**) forming an antiparallel β-sheet through intermolecular hydrogen bond.

Ac-Leu-Trp-Val-OMe (2a, 2b)

Peptide **2** differs from **1** only in the replacement of N-terminus Boc-protecting group by an Ac-group. The tripeptide, Ac-Leu-Trp-Val-OMe, crystallizes in two polymorphic forms, monoclinic $P2_1$ (**2a**) and orthorhombic $P2_12_12_1$ (**2b**) from the same solvent mixture of CH_3OH/H_2O. Interestingly, in both forms the peptide backbone conformations are extended. The molecular conformations of **2a** and **2b**, shown in Fig. 1 are dramatically different from that observed in peptide **1**. The superposition of the two polymorphs is also shown in Fig. 1. The relevant torsion angles are listed in Table 2. The peptide backbone adopts an extended conformation characteristic of a β-strand structure. The Trp side chain is also extended outward with the *trans*-conformation about the C^{α}–C^{β} bond ($\chi^1 = -176.9°$ for peptide **2a** and 172.2° for peptide **2b**). Dramatic changes in crystal state conformations of peptides upon changing the protecting group have occasionally been observed (21). Examples also exist for oligopeptides adopting completely different conformations in polymorphic crystal forms. A particularly noteworthy example is the case of [Leu^5] enkephalin (Tyr-Gly-Gly-Phe-Leu), which has been characterized in crystals in both extended (22) and β-turn (23) conformations. An interesting example of the simultaneous observation of extended and folded β-turn conformation is presented in the structure of the fully protected peptide, Boc-Leu-Dpg-Val-OMe (24) (Dpg = α,α-di-*n*-propylglycine). Undoubtedly, for the Leu-Gly-Val sequence only small energy differences separate the β-turn and extended structures. As a consequence changes in the nature of the protecting group can influence molecular packing in crystals, thereby tilting the balance between the two conformations.

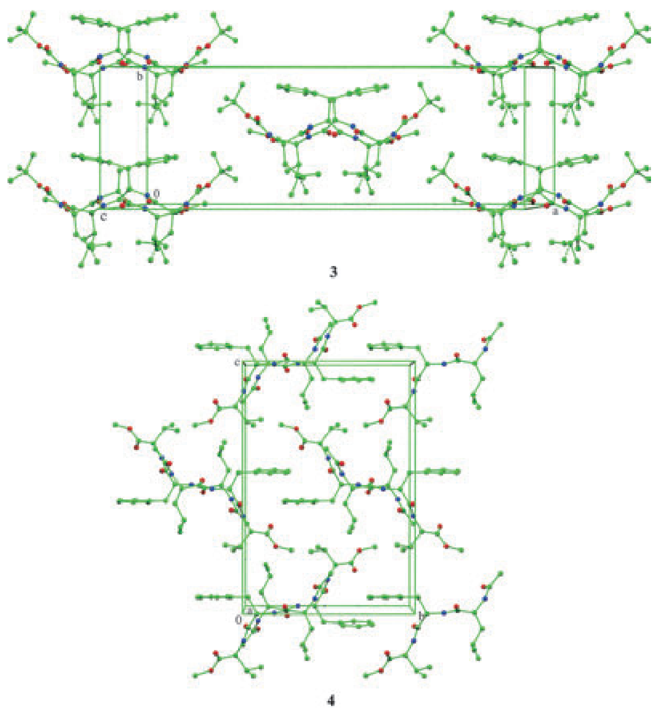

Figure 8. Another view of packing of peptide, Boc-Leu-Phe-Val-OMe (**3**) and Ac-Leu-Phe-Val-OMe (**4**), shows aromatic interactions.

Boc-Leu-Phe-Val-OMe (3)

Peptide **3**, is an analog of peptide **1**, in which the central aromatic residue is Phe instead of Trp. The backbone and side chain torsion angles are summarized in Table 2. The Leu side chain is disordered with an occupancy of C1d1 = 0.58/0.42 and C1d2 = 0.51/0.49 over two positions. The molecular conformation shown in Fig. 1 corresponds to a completely extended β-sheet conformation with all three residues adopting ϕ-, ψ-values of −120 ± 30° and 120 ± 30° respectively. Although χ^1 is fully extended (175.7°), the torsion about χ^2 (78.5°, −94.6°) folds the aromatic ring back over the Phe–Val peptide bond. A comparison of the structure of Boc-Leu-Trp-Val-OMe and Boc-Leu-Phe-Val-OMe reveals striking backbone conformational differences, which must arise as a consequence of crystal packing forces upon changing the central aromatic residue.

Ac-Leu-Phe-Val-OMe (4)

Peptide **4**, differs from peptide **3**, only in the replacement of the N-terminus Boc-protecting group by an Ac-group. The molecular conformation shown in Fig. 1, which represents a completely extended conformation. The relevant torsion angles are listed in Table 2. The structural differences between peptides **3** and **4** are mainly in the conformation of the Leu and Val side chains. Like in peptide, **3**, χ^1 is fully extended (−174.6°); the twist about χ^2 (73.7°, −107.7°), folds the aromatic ring over the Phe–Val peptide bond.

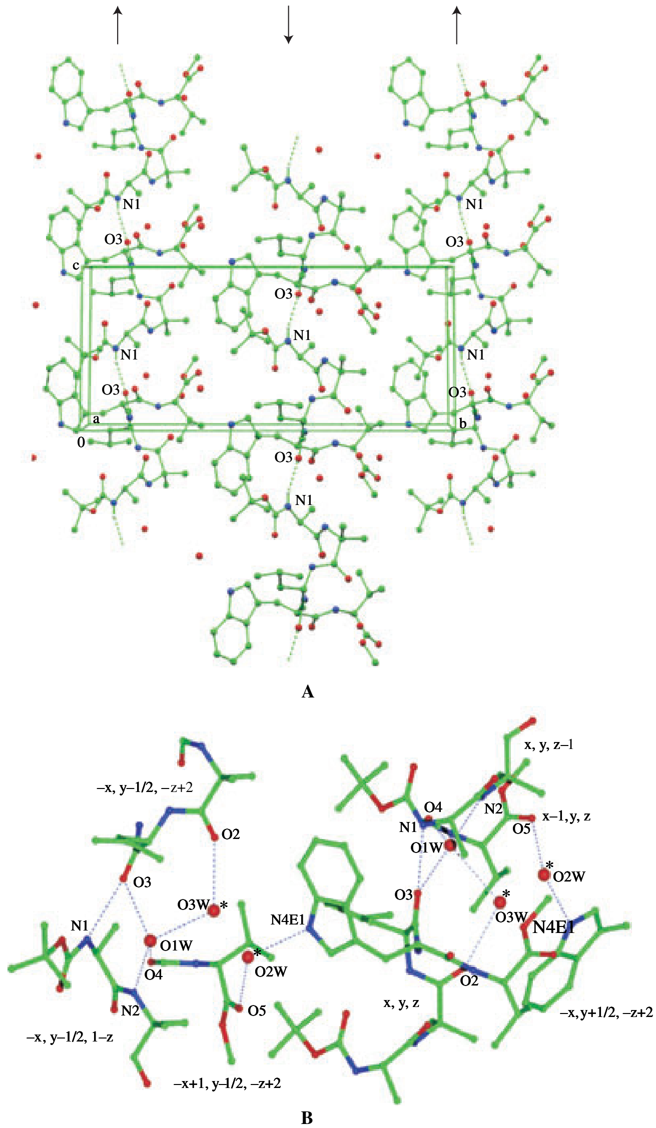

Figure 9. (A) Molecular packing of peptide, Boc-Ala-Aib-Leu-Trp-Val-OMe (**5**). (B) Solvent interactions with the molecule stabilizes the molecular packing.

Boc-Ala-Aib-Leu-Trp-Val-OMe (5)

The molecular conformation is shown in Fig. 1. The conformational angles and hydrogen bond parameters are listed in Tables 2 and 3, respectively. Peptide **5**, adopts a folded right-handed helical conformation stabilized by two intramolecular 4 → 1 hydrogen bonds [BocC(0′)…HNLeu(3) and Ala(1)C(1′)…HNTrp(4)]. The 3_{10}-helical turn encompasses

***Table 4.* List of Trp peptides from Cambridge Crystallographic Database[a]**

Sequences	Database identification number	References	Code number	Role of indole
Boc-Gly-Trp-Ala-O^{t}Bu	TUPGOA	(18)	6	Aromatic–amide interaction
Z-Aib-Trp-Aib-OMe (two molecules/asymmetric unit)	ROHVEP	(19)	7	Aromatic–amide interaction
Z-Aib-Aib-Trp-Aib-OMe	ROHVIT	(19)	8	Aromatic–aromatic interaction
Z-Aib-Aib-Aib-Trp-Aib-O^{t}Bu	ROHVOZ	(19)	9	–
Boc-Aib-Aib-Aib-Trp-Aib-OMe	ROHVUF	(19)	10	–
Boc-Aib-Trp-Leu-Aib-Ala-Leu-Aib-Ala-Phe-OMe	HICKEJ	(41)	11	Aromatic–amide interaction
Gly-Trp dihydrate	GLTRDH01	(42)	12	Aromatic–aromatic interaction
Ala-Trp monohydrate	FUJZUF	(42)	13	Aromatic–aromatic interaction
Trp-Gly monohydrate	FULGEY	(42)	14	Aromatic–aromatic interaction
Leu-Trp-Leu hydrochloride dihydrate	FUDFUF	(43)	15	Aromatic–aromatic interaction
Trp-Gly-Gly dihydrate	FIZWOA01	(44)	16	Aromatic–aromatic interaction
Trp-Gly-Leu	GUBDIQ	(45)	17	Aromatic–aromatic interaction
Trp-Met-Asp-phenylalanylamide	GASTRN10	(46)	18	Aromatic–aromatic interaction
7-Methylguanosine-5′-phosphate-Trp-Glu complex	SEKXIP10	(47)	19	Aromatic–aromatic interaction

a. The database contained 31 entries with Trp residues. Of these, only acyclic structures with short aromatic–aromatic (centroid–centroid distance between 6-membered rings of indole $\leq$ 6.5 Å) and/or aromatic–amide (centroid–centroid distance of 5-membered ring of indole and amide centroid $\leq$ 4.5 Å) distances are listed.

residues 1–3, all of which adopt ϕ-, ψ-values that lie in the α_R-region of the Ramachandran map. Formation of a turn of 3_{10}-helix is a commonly observed feature in short sequences containing the helix promoting Aib residue (24,25). The backbone dihedral angles at Trp(4) ($\phi = -123.2°$, $\psi = 4.8°$) are significantly distorted, resulting in the absence of the anticipated N(5)…O(2) hydrogen bond. The observed N(5)…O(2) distance is 4.298 Å. Water molecule O3W forms a hydrogen bond to O(2). The observed N(5)…O(1) distance 3.458 Å may be suggestive of a weak 5 → 1 interaction, although the hydrogen bond angle and O…H distances appear to be significantly distorted from values normally observed for good hydrogen bonds. The indole side chain folds back over the backbone, with a *gauche* conformation ($\chi^1 = -64.0°$) observed about the Trp C^α–C^β bond. The two water sites in the structure form bridges between exposed NH-groups including the indole side chain NH.

Crystal packing

Boc-Leu-Trp-Val-OMe (1)

Molecules of the tripeptide **1**, pack into a helical column by aggregation along the direction of crystallographic *c*-axis, shown as a stereo view in Fig. 2. Two intermolecular hydrogen bonds between Leu(1)NH…O(2)Trp(2) and indole NH…O(1)Leu(1) of a symmetry-related molecules are observed. Notably, the amide NH of the central peptide unit of the β-turn is not involved in any hydrogen bond interactions, presumably because of shielding by the indole side chain which is folded back over the peptide backbone. Inspection of the structure of the aggregated columns immediately reveals that all three hydrogen bonds run approximately parallel to the long axis of the twofold superhelix. Molecules within a column are related by a 180° rotation and translation resulting in well-defined helix faces, in which Leu/Trp and Boc/Val/OMe groups are clearly segregated. A view of three parallel superhelical columns is shown in Fig. 3. Indole rings from symmetry-related molecules are also shown between the columns. The crystal is formed by a network of aromatic–aromatic interactions between indole units on molecules related by the crystallographic 4_3 screw axis. The centroid–centroid distance for the 6-membered rings of interacting indole rings is 5.63 Å, which is well within the limits anticipated for stabilizing interactions between aromatic rings (3). Figure 4 shows two views of the packing of aromatic rings in the crystal along the crystallographic *c*-axis. The arrangement of molecules traces out a left-handed helical path as clearly seen from the projection down the *a*-axis. The crystal structure of peptide **1**, illustrates the importance of the indole side chain of Trp in promoting formation of a supramolecular right-handed helix, followed by assembly into a tetragonal space group, utilizing interactions between aromatic rings. Interestingly, crystal

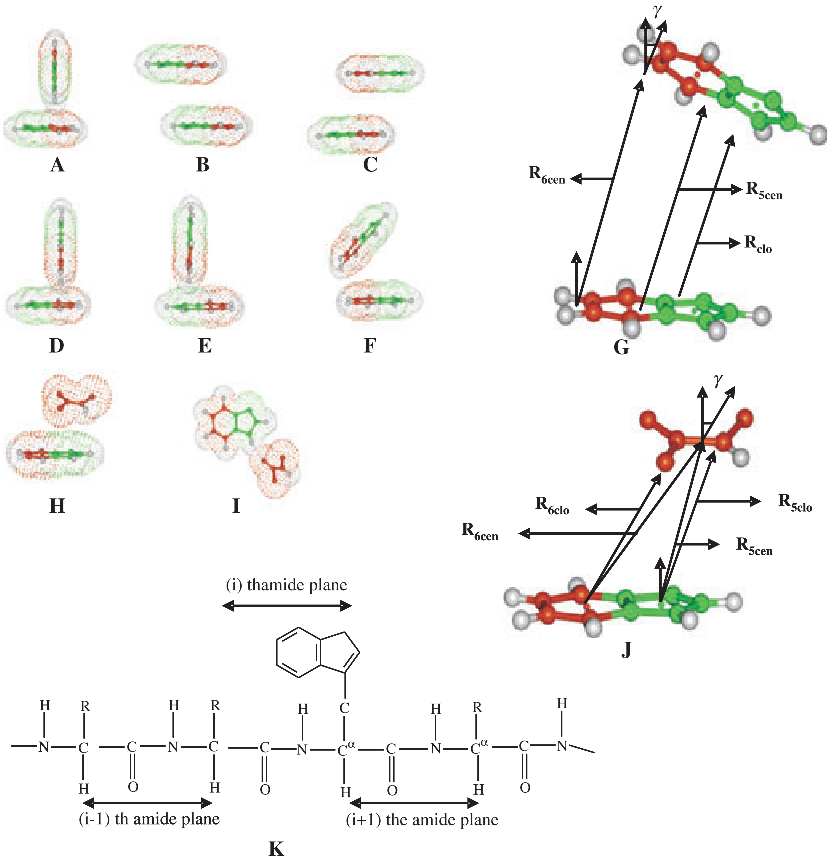

Figure 10. (A) The indole rings are placed at a centroid–centroid distance of 5.5 Å. The van der Waals surfaces generated with attached hydrogen atoms are indicated: (A) NH…π, involving the indole NH and the 6-membered ring; (B and C) two possible parallel displacement arrangement; (D and E) two possible orientations of perpendicular arrangement; (F) inclined orientation. Parameters used to define the aromatic interactions are shown in (g): R_{5cen} (Å) is the distance between the centroid of 5-membered rings and R_{6cen} (Å) is the distance between the centroid of 6-membered rings; γ (deg) is the interplaner angle; R_{clo} (Å) is the shortest distance between two heavy atoms of the interacting rings. (B) The centroid–centroid distance of the amide plane and 5-membered ring is 4.5 Å. (H) Stacked arrangement of indole and amide plane; (I) hydrogen bonds between proximal amide and indole group. Parameters used to define the aromatic–amide interactions are shown in (J): R_{5cen} (Å) is the centroid–centroid distance of 5-membered ring and amide centroid; R_{6cen} (Å) is the centroid–centroid distance of 6-membered ring and amide centroid; γ (deg) is the interplaner angle; R_{5clo} (Å) is the shortest distance between the 5-membered centroid and the closest heavy atom of amide plane; R_{6clo} (Å) is the shortest distance between the 6-membered centroid and the closest heavy atom of amide plane. (K) Schematic representation of aromatic–amide interaction where aromatic side chain placed in *i*th position interacting with $(i-1)$th or $(i+1)$th amide planes within the peptide backbone.

of peptide **1**, were also grown from the mixture of ethanol/water, and 1 : 2 methanol/water. The solvent mixture 1 : 2 methanol/water was used to incorporate water molecule into the crystal. But all the cases, the crystals belonged to the primitive tetragonal crystal system, with exactly same cell parameters suggesting that the superhelical assembly appeared to be a favored packing mode. The importance of Trp side chains in participating in both hydrogen bonding and aromatic interactions in the context of protein structures has been emphasized (14). The formation of the superhelix, facilitated by both backbone and side chain hydrogen bonds, has passed unnoticed in the crystal structure of a conformationally similar tripeptide, Z-Aib-Trp-Aib-OMe (20). In that case, crystal formation does not involve indole–indole interactions. The cooperative role of weak interactions in determining molecular assemblies in crystals has been emphasized in several recent examples (27–29).

Ac-Leu-Trp-Val-OMe (2a and 2b)

In both crystals, **2a** and **2b**, molecules pack into antiparallel β-sheet structures. The potential hydrogen bond parameters are listed in Table 3. Three intermolecular hydrogen bonds, Leu(1)NH…OCTrp(2); Trp(2)NH…OCLeu(1); and Val(3)NH…OCAc(0) between symmetry-related molecules form the infinite sheet. The fourth hydrogen bond between the indole NH- and Val(3)CO-group links molecules in adjacent columns shown in Fig. 5. There is little difference of the intermolecular hydrogen bonding modes between the two polymorphs. Figure 6 shows an alternate view of the packing, which illustrates the close approach of aromatic

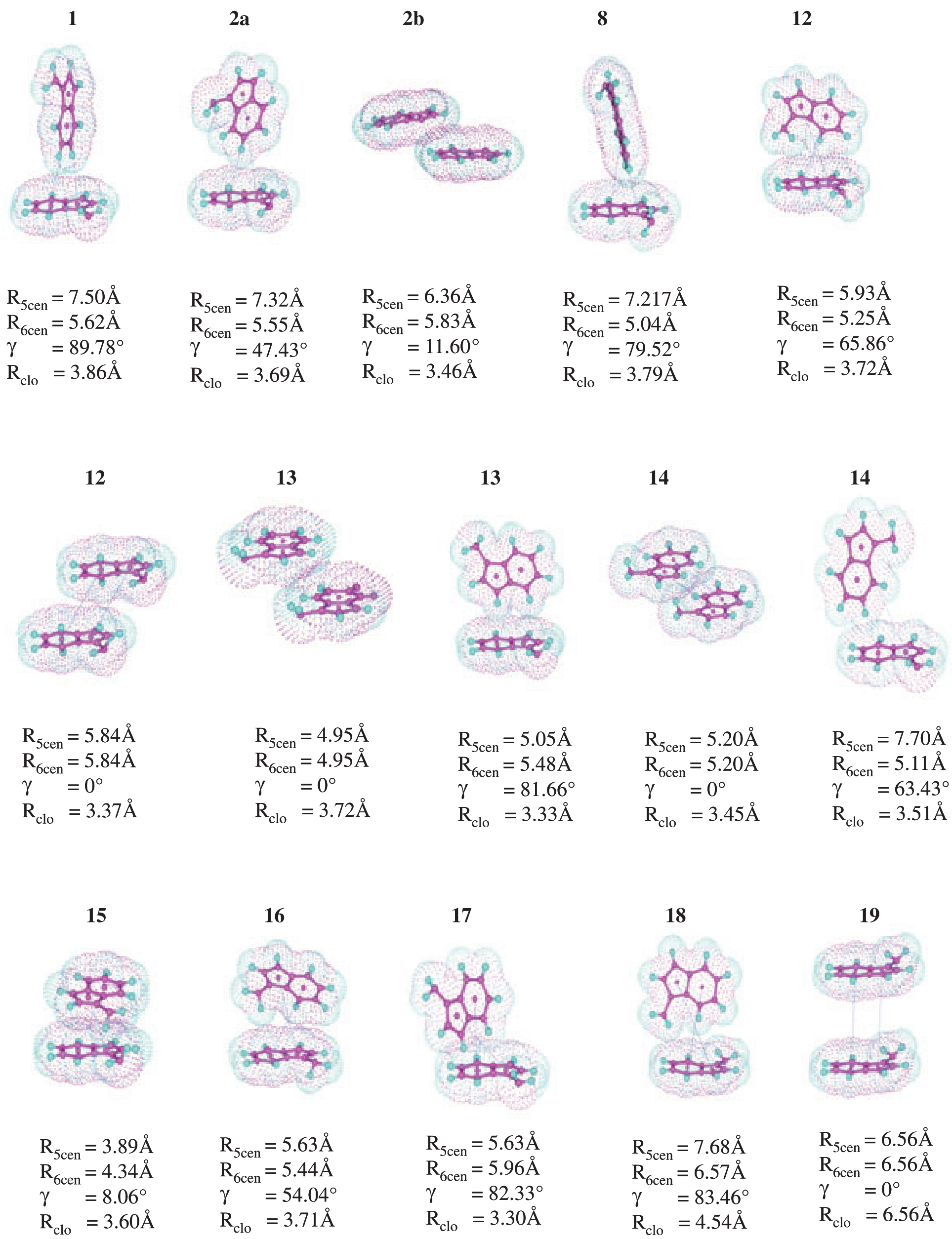

Figure 11. Aromatic–aromatic interactions observed in the crystals of peptides. The van der Waals surfaces are shown. The parameters R_{5cen}, R_{6cen}, γ and R_{clo} are indicated.

rings on neighboring molecules. In both polymorphs, indole rings stack in pairs with a significant difference in the orientation of the rings in the two cases. In peptide **2a**, the interplaner angle is 47° and the distance between the centroids of the 6-membered rings is 5.55 Å, whereas in peptide **2b**, the interplaner angle is 11° and the distance between the centroids of 6-membered rings is 5.84 Å.

Boc-Leu-Phe-Val-OMe (3) and Ac-Leu-Phe-Val-OMe (4)

Peptides **3** and **4**, which contain Phe at the second position may be contrasted with peptides **1** and **2**, which contain a Trp residue at that position. Both peptides adopt extended conformations, packing into an antiparallel β-sheet arrangement in crystals. All relevant distances and angular parameters between potential hydrogen bond donor and acceptor groups are summarized in Table 3. Strips of β-sheet are brought together by van der Waals interactions, as shown in Fig. 7. An alternative view of the packing shown in Fig. 8 reveals significant differences in packing of aromatic side chains. In peptide **3**, no aromatic–aromatic interactions are observed whereas, in peptide **4**, the rings are stacked in pairs with an interplaner angle of 64.78° and a centroid–centroid distance of 5.80 Å.

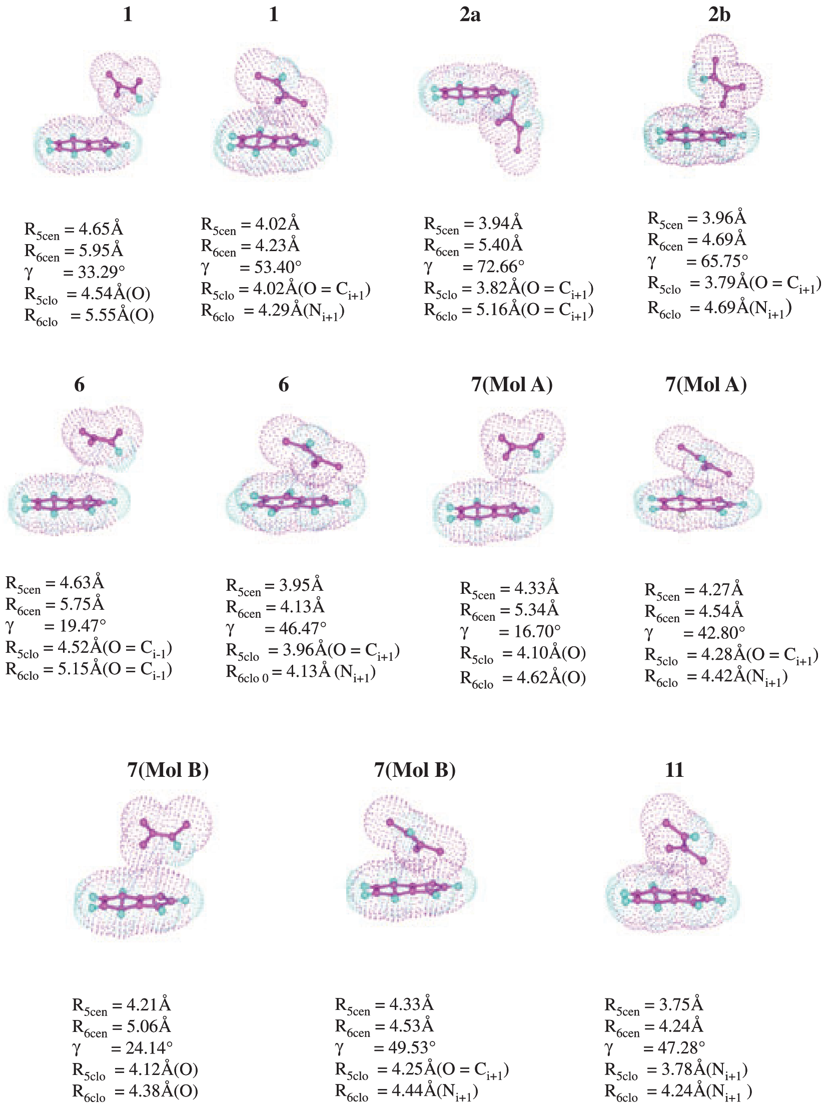

Figure 12. Aromatic–amide interactions observed in the crystals of peptides. The van der Waals surfaces are shown. The parameters R_{5cen}, R_{6cen}, γ and R_{5clo}, R_{6clo} are indicated.

Boc-Ala-Aib-Leu-Trp-Val-OMe (5)

The packing of the helical peptide **5**, into crystals is facilitated by bridging water molecules. As many as three water sites are observed. While site O1W shows full occupancy, O2W and O3W show half occupancy with simultaneous occupancy being sterically excluded (O2W…O3W = 2.260 Å) (29). O2W forms a hydrogen bond with an indole NH-group and the Val(5)CO-group. O3W bridges O1W and the Aib(2)CO-group. O1W forms four hydrogen bonds acting as a donor in two and acting as an acceptor in two cases, shown in Fig. 9. All the hydrogen bond parameters are summarized in Table 3. Notably, the potential helical intramolecular hydrogen bond involving Val(5)NH is distorted by the hydrogen bond interaction to O3W. This is also evident in the large deviation of the backbone dihedral angle of Trp ($\phi = -123.2°$, $\psi = 4.8°$) from that anticipated in a helix.

Interactions involving the indole ring of Trp

Aromatic–aromatic and aromatic–amide interactions have been suggested to be important determinants of folded structures of proteins. There have been several detailed analyses of interactions involving Phe rings in peptides and proteins (31–33) and interactions between the aromatic ring and the backbone amide group within a protein environment (34–36). The indole ring of Trp has been the focus of several theoretical studies (37–41). The analysis of indole–indole interactions in proteins is limited by the relatively low occurrence of Trp–Trp pairs in globular proteins. The determination of several peptide structures with Trp residues in this study promoted us to examine the modes of interaction of indole side chains. Table 4 provides a list of Trp-containing peptides (19,20,42–48) from the Cambridge Crystallographic Database, which

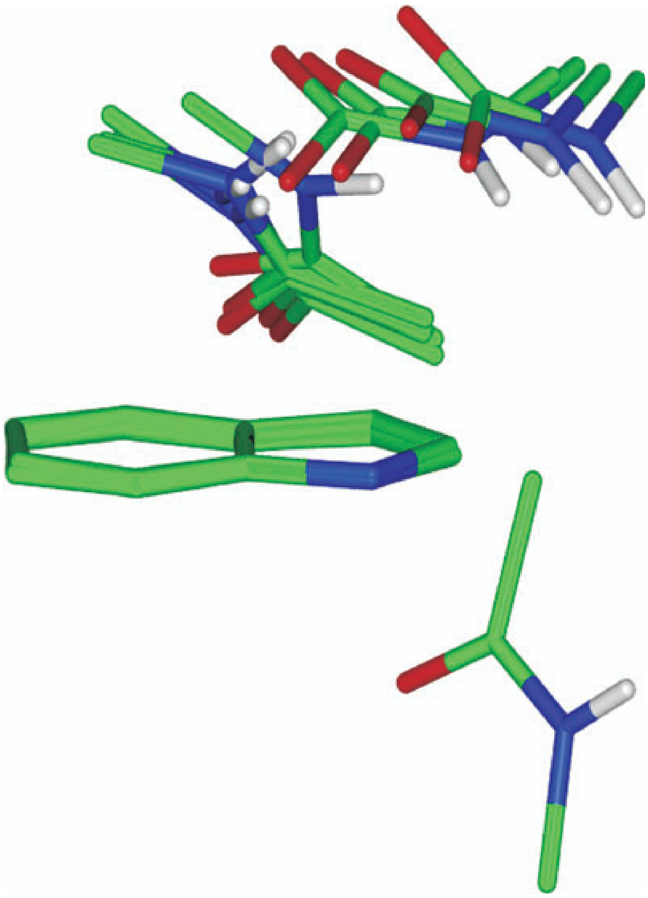

Figure 13. Schematic representation of environment of amide planes surrounding the indole ring which provides the stabilizing aromatic–amide interactions. The representation was generated using the program MOLMOL (50).

have been used in addition to the structures determined in the present study. Figure 10 schematically represents the common idealized arrangements of indole rings and defines the interaction parameters used to describe ring orientations. The experimental values determined are summarized in Fig. 11. In the case of Trp–Trp interactions there is a fairly wide distribution of the interplaner angle γ, while several examples of almost parallel and perpendicular arrangements are observed. Close approach of the 6-membered ring appears to be favorable with $R_{6cen} < R_{5cen}$ in most cases. Figure 12 summarizes the observed aromatic–amide interactions. In all the cases of extended backbone conformations of Trp, the aromatic group is proximal to the peptide unit formed with the succeeding amino acid. In the case of peptides **1**, **6**, and **7**, the indole ring is within interaction distance, with both preceding and succeeding peptide bonds. In all cases, the distances from the amide unit to the 5-membered are shorter than the 6-membered ring. There are no examples in the data set for any potential NH…π interactions. Figure 13 schematically summarizes the disposition of interacting amide units with respect to the partner indole ring.

Conclusions

No strongly preferred orientation of two interacting indole rings has emerged in the examples considered in the present study. This may be suggestive of a relatively broad potential well in which small changes of orientation do not significantly affect the interaction energies. Such a situation has been suggested for interacting Phe-groups from theoretical calculations (49) and supported by experimental studies on Phe-rich peptides (50). Theoretical studies suggest that aromatic–amide interactions may contribute as much as about 4 kcal/mol toward net stabilization (4). The present analysis of Trp-amide orientation from crystal structures does support preferred orientations in which the indole and amide planes subtend a small interplaner angle. It must of course be stressed that orientations of the Trp-indole ring with respect to the preceding and succeeding units are limited by the torsions about the C^{α}–C^{β} and C^{β}–C^{γ} bonds, in addition to the local backbone conformation.

Acknowledgements: This work is supported by grants from the Council of Scientific and Industrial Research, India and program support in the area of Molecular Diversity and Design, Department of Biotechnology, India. R.M. is supported by the award of a Junior Research Fellowship from the Council of Scientific and Industrial Research, India. The CCD diffractometer facility is supported under the IRHPA program of the Department of Science and Technology, Government of India.

References

1. Burley, S.K. & Petsko, G.A. (1986) Amino-aromatic interactions in proteins. *FEBS Lett.* **203**, 139–143.
2. Pejov, L. (2001) A gradient-corrected density functional study of indole self-association through N-H…π hydrogen bonding. *Chem. Phys. Lett.* **339**, 269–278.
3. Burley, S.K. & Petsko, G.A. (1985) Aromatic-aromatic interaction: a mechanism of protein structure stabilization. *Science* **229**, 23–28.

4. Duan, G., Smith, V.H. Jr & Weaver, D.F. (1999) An ab initio and data mining study on aromatic-amide interactions. *Chem. Phys. Lett.* **310**, 323–332.
5. Tóth, G., Murphy, R.F. & Lovas, S. (2001) Investigation of aromatic-backbone amide interactions in the model peptide acetyl-Phe-Gly-Gly-N-methyl amide using molecular dynamics simulations and protein database search. *J. Am. Chem. Soc.* **123**, 11782–11790.
6. Schiffer, M., Chang, C.-H. & Stevens, F.J. (1992) The function of tryptophan residues in membrane proteins. *Protein Eng.* **5**, 213–214.
7. Hu, W., Lee, K.-C. & Cross, T.A. (1993) Tryptophans in membrane proteins: indole ring orientations and functional implications in the gramicidin channel. *Biochemistry* **32**, 7035–7047.
8. Hu, W. & Cross, T.A. (1995) Tryptophan hydrogen bonding and electric dipole moments: functional roles in the gramicidin channel and implications for membrane proteins. *Biochemistry* **34**, 14147–14155.
9. Yau, W.-M., Wimley, W.C., Gawrisch, K. & White, S.H. (1998) The preference of tryptophan for membrane interfaces. *Biochemistry* **37**, 14713–14718.
10. Woolf, T.B., Grossfield, A. & Pearson, J.G. (1999) Indoles at interfaces: calculations of electrostatic effects with density functional and molecular dynamics methods. *Int. J. Quantum Chem.* **75**, 197–206.
11. Baldwin, R.L. (2002) Making a network of hydrophobic clusters. *Science* **295**, 165–166.
12. Cochran, A.G., Skelton, N.J. & Starovasnik, M.A. (2001) Tryptophan zippers: stable, monomeric β-hairpins. *Proc. Natl Acad. Sci. U S A* **98**, 5578–5583.
13. Samanta, U., Pal, D. & Chakrabarti, P. (1999) Packing of aromatic rings against tryptophan residues in proteins. *Acta Crystallogr.* **D55**, 1421–1427.
14. Samanta, U., Pal, D. & Chakrabarti, P. (2000) Environment of tryptophan side chains in proteins. *Proteins: Struct., Funct. Genet.* **38**, 288–300.
15. Thomas, A., Meurisse, R., Charloteaux, B. & Brasseur, R. (2002) Aromatic side-chain interactions in proteins: I. Main structural features. *Proteins: Struct., Funct. Genet.* **48**, 628–634.
16. Sheldrick, G.M. SHELXS-97 (1997) *Program for the Solution of Crystal Structures*. University of Göttingen, Göttingen, Germany.
17. Sheldrick, G.M. SHELXL-97 (1997) *Program for the Refinement of Crystal Structures*. University of Göttingen, Göttingen, Germany.
18. Anthoni, U., Christophersen, C., Flensburg, C., Jakobsen, M.H., Jensen, J. & Nielsen, P.H. (1996) Tryptophan-derived peptides: 1. Crystal structure and solution conformation of Boc-Gly-Trp-Ala-O^{t}Bu. *Struct. Chem.* **7**, 103–110.
19. George, C., Flippen-Anderson, J.L., Bianco, A., Crisma, M., Formaggio, F. & Toniolo, C. (1996) Crystallographic characterization of tryptophan-containing peptide 3_{10}-helices. *Pept. Res.* **9**, 315–321.
20. Evans, M.C., Pradhan, A., Venkatraman, S., Ojala, W.H., Gleason, W.B., Mishra, R.K. & Johnson, R.L. (1999) Synthesis and dopamine receptor modulating activity of novel peptidomimetics of $_L$-Prolyl-$_L$-Leucyl-glycinamide featuring α,α-disubstituted amino acids. *J. Med. Chem.* **42**, 1441–1447.
21. Karle, I.L. & Karle, J. (1983) [Leu^5] enkephalin: four cocrystallizing conformers with extended backbones that form an antiparallel β-sheet. *Acta Crystallogr.* **B39**, 625–637.
22. Smith, G.D. & Griffin, J.F. (1978) Conformation of [Leu^5] enkephalin from X-ray diffraction: features important for recognition at opiate receptor. *Science* **199**, 1214–1216.
23. Prasad, S., Mitra, S., Subramanian, E., Velmurugan, D., Balaji Rao, R. & Balaram, P. (1994) Coexistence of folded and extended conformations of tripeptide containing α,α-Di-n-propylglycine in crystals. *Biochem. Biophys. Res. Commun.* **198**, 424–430.
24. Prasad, B.V. V. & Balaram, P. (1984) The stereochemistry of peptides containing alpha-aminoisobutyric acid. *CRC Crit. Rev. Biochem.* **16**, 307–348.
25. Karle, I.L. & Balaram, P. (1990) Structural characteristics of α-helical peptide molecules containing Aib residues. *Biochemistry* **29**, 6747–6756.
26. Halder, D., Maji, S.K., Sheldrick, W.S. & Banerjee, A. (2002) First crystallographic signature of the highly ordered supramolecular helical assemblage from a tripeptide containing a non-coded amino acid. *Tetrahedron Lett.* **43**, 2653–2656.
27. Halder, D., Maji, S.K., Drew, M.G.B., Banerjee, A. & Banerjee, A. (2002) Self-assembly of a short peptide monomer into a continuous hydrogen bonded supramolecular helix: the crystallographic signature. *Tetrahedron Lett.* **43**, 5465–5468.
28. Maji, S.K., Banerjee, A., Drew, M.G.B., Halder, D. & Banerjee, A. (2002) Self-assembly of a tetrapeptide in which a unique supramolecular helical structure is formed via intermolecular hydrogen bonding in the solid state. *Tetrahedron Lett.* **43**, 6759–6762.
29. Aravinda, S., Shamala, N., Das, C. & Balaram, P. (2002) Structural analysis of peptide helices containing centrally positioned lactic acid. *Biopolymers* **64**, 255–267.
30. Burley, S.K. & Petsko, G.A. (1986) Dimerization energetics of benzene and aromatic amino acid side chains. *J. Am. Chem. Soc.* **108**, 7995–8001.
31. Burley, S.K. & Petsko, G.A. (1988) *Adv. Protein Chem.* **39**, 125–189.
32. Aravinda, S., Shamala, N., Das, C., Sriranjini, A., Karle, I.L. & Balaram, P. (2003) Aromatic-aromatic interactions in crystal structures of helical peptide scaffolds containing phenylalanine residues. *J. Am. Chem. Soc.* **125**, 5308–5315.
33. Tóth, G., Watts, C.R., Murphy, R.F. & Lovas, S. (2001) Significance of aromatic-backbone amide interactions in protein structure. *Proteins: Struct., Funct. Genet.* **43**, 373–381.
34. Duan, G., Smith, V.H. Jr & Weaver, D.F. (2000) A data mining and ab initio study of the interaction between the aromatic and backbone amide groups in proteins. *Int. J. Quantum Chem.* **80**, 44–60.
35. Duan, G., Smith, V.H. Jr & Weaver, D.F. (2000) Characterization of aromatic-amide (side-chain) interactions in proteins through systematic ab initio calculations and data mining analyses. *J. Phys. Chem. A* **104**, 4521–4532.
36. Gervasio, F.L., Chelli, R., Procacci, P. & Schettino, V. (2002) The nature of intermolecular interactions between aromatic amino acid residues. *Proteins: Struct., Funct. Genet.* **48**, 117–125.
37. Separovic, F., Ashida, J., Woolf, T., Smith, R. & Terao, T. (1999) Determination of chemical shielding tensor of an indole carbon and application to tryptophan orientation of a membrane peptide. *Chem. Phys. Lett.* **303**, 493–498.
38. Sobolewski, A. & Domcke, W. (1999) Ab initio investigations on the photophysics of indole. *Chem. Phys. Lett.* **315**, 293–298.
39. Callis, P.R. & Vivian, J.T. (2003) Understanding the variable fluorescence quantum yield of tryptophan in proteins using QM-MM simulations. Quenching by charge transfer to the peptide backbone. *Chem. Phys. Lett.* **369**, 409–414.
40. Bingham, N.C., Smith, N.E.C., Cross, T.A. & Busath, D.D. (2003) Molecular dynamics simulations of Trp side-chain conformational flexibility in the gramicidin A channel. *Biopolymers (Pept. Sci.)* **71**, 593–600.

41. Karle, I.L., Flippen-Anderson, J.L., Gurunath, R. & Balaram, P. (1994) Facile transition between 3_{10}- and α-helix: structures of 8-, 9-, and 10-residue peptides containing the-(Leu-Aib-Ala)$_2$-Phe-Aib-fragment. *Protein Sci.* **3**, 1547–1555.
42. Emge, T.J., Agrawal, A., Dalessio, J.P., Dukovic, G., Inghrim, J.A., Janjua, K., Macaluso, M., Robertson, L.L., Stiglic, T.J., Volovik, Y. & Georgiadis, M.M. (2000) Alaninyltryptophan hydrate, glycyltryptophan dihydrate and tryptophylglycine hydrate. *Acta Crystallogr.* **C56**, e469–e471.
43. Wu, S., Declercq, J.P., Tinant, B. & Meerssche, M.V. (1987) Crystal structure and conformation of short linear peptides: Part VIII. L-leucyl-L-tryptophanyl-L-leucine hydrochloride dihydrate. *Bull. Soc. Chim. Belg.* **96**, 581–586.
44. Subramanian, E. & Sahayamary, J.J. (1989) Structure and conformation of linear peptides. *Int. J. Pept. Protein Res.* **34**, 134–138.
45. Asai, Y., Nonaka, N., Nishio, M., Okamura, K., Date, T., Sugita, T., Ohnuki, T. & Komatsubara, S. (1997) TMC-2A, -2B and -2C, new dipeptidyl peptidase IV inhibitors produced by *Aspergillus oryzae* A374. *J. Antibiot.* **50**, 653–658.
46. Cruse, W.B.T., Egert, E., Viswamitra, M.A. & Kennard, O. (1982) The structure of the hydrochloride salt of Trp-Met-Asp-Phe-$NH_2.CH_3OH.0.5C_2H_5OC_2H_5$, the C-terminal tetrapeptide amide of gastrin. *Acta Crystallogr.* **B38**, 1758–1764.
47. Ishida, T., Iyo, H., Ueda, H., Doi, M., Inoue, M., Nishimura, S. & Kitamura, K. (1991) Interaction of indole derivatives with biologically important aromatic compounds. Importance of simultaneous co-operation of hydrogen-bond pairing and stacking interactions for recognition of guanine base by a peptide: X-ray crystal analysis of 7-methylguanosine-5′-phosphate-tryptophanylglutamic acid complex. *J. Chem. Soc. Perkin Trans.* **1**, 1847–1853.
48. Sun, S. & Bernstein, E.R. (1996) Aromatic van der Waals clusters: structure and non-rigidity. *J. Phys. Chem.* **100**, 13348–13366.
49. McGaughey, G.B., Gagnes, M. & Rappe, A.K. (1998) π-Stacking interactions alive and well in proteins. *J. Biol. Chem.* **273**, 15458–15463.
50. Koradi, R., Billeter, M. & Wuthrich, K. (1996) MOLMOL: a program for display and analysis of macromolecular structures. *J. Mol. Graph.* **14**, 51–55.